periodically spaced crystallographic shear (CS) planes. The CS planes delimit quasi two-dimensional blocks of the perovskite structure with a thickness of (*n*-2) BO_6 octahedra, *n* being the number of the homologue in the series.

Using the appropriate chemical composition and thermal treatment conditions we have isolated in a single phase form different members of the homologous series with $n = 4$ ($Pb_{4-2x}A_{2x}Fe_4O_{10}$ (A = Sr, Ba)), $n = 5$ ($Pb_{2.9}Ba_{2.1}Fe_4TiO_{13}$, $Pb_2Ba_2BiFe_5O_{13}$), $n = 6$ ($Pb_{3.8}Bi_{0.2}Ba_2Fe_{4.2}Ti_{1.8}O_{16}$, $PbBaBiFe_3O_8$) and $n = 7$ ($Pb_{4.5}Bi_{0.2}Ba_{2.4}Fe_{4.9}Ti_{2.1}O_{19}$) [1], [2].

The crystal structures of the obtained compounds have been determined using a combination of diffraction and electron microscopy techniques: X-ray (XRD) and neutron powder diffraction (NPD), electron diffraction (ED), and high angle annular dark field scanning transmission electron microscopy (HAADF-STEM). The compounds crystallize in an orthorhombic crystal system with the lattice parameters $a \approx a_p\sqrt{2}$, $b \approx b_p$, $c \approx 9.7\text{Å} + (n-2)a_p\sqrt{2}$, where $a_p \approx 4.06$Å. The space groups are *Pnma*, *Ammm* and *Imma* for the 4th, 5th and 6th members, respectively. The $A_nB_nO_{3n-2}$ structures can be represented as a sequence of atomic layers $-ABO-(O_2-ABO)_{n-2}-O_2-ABO-ABO-(O_2-ABO)_{n-2}-O_2-ABO-$. HAADF-STEM reveals a long range ordered sequence of the perovskite modules with a uniform thickness for members with $n = 4$–6.

In this type of structures, the cations are partially ordered. At the CS planes, tunnels are created in which only the lead and bismuth cations are situated. The formation of tunnels allows the spatial accommodation of the lone electron pair of these cations. The coordination number of the B cations at the CS planes is 5 and these BO_5 tetragonal pyramids are occupied exclusively by Fe^{3+} cations. The remaining Fe^{3+} cations as well as Ti^{4+} cations are located in the BO_6 octahedra of the perovskite modules. The CS planes introduce edge sharing connections of the transition metal-oxygen polyhedra at the interface between the perovskite blocks. This results in intrinsically frustrated magnetic couplings between the perovskite blocks due to a competition of the exchange interactions between the edge- and the corner-sharing metal-oxygen polyhedra.

[1] I. Nikolaev, H. D'Hondt, A. Abakumov, A. Balagurov, I. Bobrikov, D. Sheptyakov, V. Pomjakushin, K. Pokholok, D. Filililmonov, G. Van Tendeloo, E. Antipov, *Phys. Rev. B* **2008**, *78*, 024426. [2] A. Abakumov, J. Hadermann, M. Batuk, H. D'Hondt, O. Tyablikov, M. Rozova, K. Pokholok, D. Filimonov, D. Sheptyakov, A. Tsirlin, D. Niermann, J. Hemberger, G. Van Tendeloo, E. Antipov, *Inorganic Chemistry* **2010**, *49 (20)*, 9508–9516.

Keywords: perovskite, homologous_series, lead

MS79.P03

Acta Cryst. (2011) A**67,** C693

Electron crystallography based on inverse dynamic scattering

Kurt Scheerschmidt, *Max Planck Institut für Mikrostrukturphysik, Weinberg 2, Halle-Saale (Germany).* E-mail: schee@mpi-halle.de

Electron crystallography and electron microscope tomography may enhance structure investigations via local object analysis. However, this has in contrast to X-ray techniques the disadvantage, that an ill-posed inverse problem for the highly nonlinear dynamical theory has to be solved. Fig. 1 schematically shows all necessary steps of the object analysis: anticlockwise the trial-and-error technique, clockwise the direct solution of the inverse problem. Authors which proposed partial solutions are listed, too. Details are be found in [1] with respective references. In [1], [2] also a special solution of the inverse problem for the local parameter analysis is given. Step 1 of the inversion is solved, by replacing the image by a hologram or a defocus series, which makes the problem linear, and finding the exit object wave by inverse Fourier transform. Step 2 yielding the object structure directly from the exit wave, is the real challenge of inversion. Step 3, the analysis of lattice defects, has no explicit solution yet.

The solution proposed here for step 2 can be characterized in short as follows [1], [2]: The first step of inversion yield the moduli and phases for all reflections of the experimental exit plane waves Φ^{exp} as function of lateral (pixel) positions (i,j). Theoretical waves Φ^{th} are then calculated using the dynamical scattering matrix $\mathbf{M}$ for an a priori model characterized by the number of beams and the scattering potential $\mathbf{V}$. With a suitable experimentally predetermined a priori beam orientation $\mathbf{K}_o$ and sample thickness t_o as a free parameter, a perturbation approximation yields both Φ^{th} and $\mathbf{M}$ as linear functions of the parameter to be retrieved. Its analytic form enables the inverse solution of $\|\Phi^{exp}-\Phi^{th}\|$=Min yielding directly for each image pixel the local thickness t(i,j), the local beam orientation **K**(i,j), and further data of the parameter space.

The linearization transforms the ill-posed problem to a well posed one and enables the analytic inverse. However, the solution is ill-conditioned. With the generalized and regularized inverse in [2] an enhancement of the solution is given. By applying second order perturbation and using a mixed type potential $\mathbf{V}(i,j) = q_k(i,j)\ \mathbf{V}^k$ in [1] with the parameters $q_k(i,j)$ also local potential variations can be retrieved [3]. Smoothing, coupling of different parameters via additional a priori information, including the iteration of the start values, if the retrieved parameter go beyond the confidence region, finally help to avoid modeling errors.

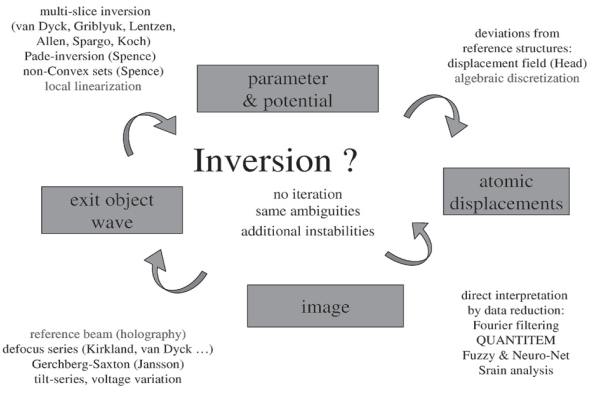

[1] K. Scheerschmidt, *Ultramicroscopy* **2010,** *110*, 543-547. [2] K. Scheerschmidt *Journal of Microsc,* **1998,** *190*, 238-248. [3] K. Scheerschmidt *Proc. 17. Int. Microsc. Congr. Brazil* **2010,** *I8.4*.

Keywords: inverse problems, electron holography, analytic approximation

MS79.P04

Acta Cryst. (2011) A**67,** C693-C694

Automatic diffraction tomography (ADT) with precession on 6H-SiC and NiTe

Enrico Mugnaioli,[a] Eleni Sarakinou,[b] Christos Lioutas,[b] Nikolaos Vouroutzis,[b] Nikolaos Frangis,[b] Ute Kolb,[a] Stavros Nicolopoulos,[c] [a]*Institut for Physical Chemistry, Johannes Gutenberg -University, Welderweg 11, 55099 Mainz (Germany).* [b]*Department of Physics, Aristotle University of Thessaloniki, 54124 Thessaloniki, (Greece).* [c]*NanoMEGAS SPRL, Blvd Edmond Machtens 79, B-1080 Brussels, (Belgium).* E-mail: mugnaiol@uni-mainz.de

Automated electron Diffraction Tomography (ADT) in combination with precession electron diffraction (PED) has been recently used in the investigation of nano-crystalline materials. By the use of this method